THE JOURNAL OF PHYSICAL CHEMISTRY B

pubs.acs.org/JPCB Article

Influence of Ionic Strength on Hydrophobic Interactions in Water: Dependence on Solute Size and Shape

Małgorzata Bogunia and Mariusz Makowski*

Cite This: *J. Phys. Chem. B* 2020, 124, 10326–10336

Read Online

ACCESS | Metrics & More | Article Recommendations | Supporting Information

ABSTRACT: Hydrophobicity is a phenomenon of great importance in biology, chemistry, and biochemistry. It is defined as the interaction between nonpolar molecules or groups in water and their low solubility. Hydrophobic interactions affect many processes in water, for example, complexation, surfactant aggregation, and coagulation. These interactions play a pivotal role in the formation and stability of proteins or biological membranes. In the present study, we assessed the effect of ionic strength, solute size, and shape on hydrophobic interactions between pairs of nonpolar particles. Pairs of methane, neopentane, adamantane, fullerene, ethane, propane, butane, hexane, octane, and decane were simulated by molecular dynamics in AMBER 16.0 force field. As a solvent, TIP3P and TIP4PEW water models were used. Potential of mean force (PMF) plots of these dimers were determined at four values of ionic strength, 0, 0.04, 0.08, and 0.40 mol/dm^3, to observe its impact on hydrophobic interactions. The characteristic shape of PMFs with three extrema (contact minimum, solvent-separated minimum, and desolvation maximum) was observed for most of the compounds for hydrophobic interactions. Ionic strength affected hydrophobic interactions. We observed a tendency to deepen contact minima with an increase in ionic strength value in the case of spherical and spheroidal molecules. Additionally, two-dimensional distribution functions describing water density and average number of hydrogen bonds between water molecules were calculated in both water models for adamantane and hexane. It was observed that the density of water did not significantly change with the increase in ionic strength, but the average number of hydrogen bonds changed. The latter tendency strongly depends on the water model used for simulations.

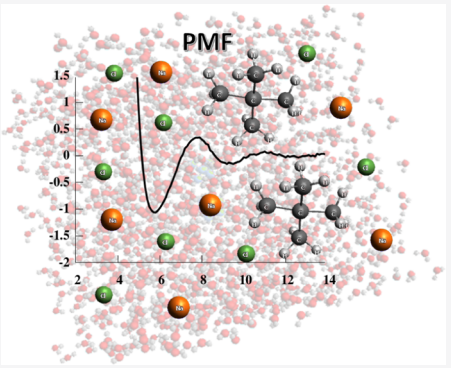

INTRODUCTION

Hydrophobicity is a property of considerable importance in biology, chemistry, and biochemistry. It is defined as low affinity for water or even the avoidance of water by certain molecules or substances. Hydrophobic interactions refer to water-mediated interactions of hydrophobic particles in an aqueous environment, and these interactions are involved in many processes in an aqueous solution, particularly complexation, surfactant aggregation, and coagulation.[1,2] Hydrophobic interactions also play a crucial role in the formation and stability of proteins, biological membranes, and micelles. Hydrophobic effects have a significant effect on molecular recognition, detergency, and formation of gas clathrates.[1,3−5] It is hypothesized that hydrophobic interactions play a pivotal role in the initiation of protein-folding process.[6−8] It is assumed that one of the initial steps of this process occurs in the protein fragment with the greatest number of nonpolar residues and that hydrophobic interactions lead to protein folding.[6−8]

When hydrophobic interactions occur, van der Waals interactions take place between nonpolar compounds and some specific changes in water structure. Once the molecules come closer to each other, the number of water particles in contact with them decreases. Moreover, these structural changes significantly contribute to free energy.[1] Hydrophobic interactions are categorized as solvent-induced interactions.[3,5,9] In this context, hydrophobicity could be characterized by the free energy of association or alternatively by changes in the free energy as a function of the distance between a pair of nonpolar molecules in an aqueous solution.[1,3]

Experimental techniques such as X-ray or neutron scattering and other measurements provide some thermodynamic data for determining hydrophobicity.[10−16] Experimental methods, however, encounter difficulties because of low solubility of nonpolar substances in water, except for a homologous series of compounds with nonpolar tails and polar heads.[1] Because of these issues, hydrophobic interactions cannot be measured directly. Hence, computational methods are widely used to study this property.[2,3]

Received: July 13, 2020
Revised: October 20, 2020
Published: November 4, 2020

https://dx.doi.org/10.1021/acs.jpcb.0c06399
J. Phys. Chem. B 2020, 124, 10326−10336

The size and shape of interacting particles and temperature have a significant effect on hydrophobicity. Around room temperature, the entropy contribution prevails in hydrophobic effects for small molecules, but for larger ones, the enthalpic term is dominant. The solubility of small nonpolar particles in water decreases with increasing temperature and increases with the decline in temperature. Moreover, the entropy term is less significant than the energetic one at higher temperatures.[2,17−19] Extensive research has been conducted on the relationship between hydrophobicity and temperature as well as between hydrophobicity and the size of nonpolar particles. The hydrophobic effect is greater for large molecules than for small ones because of the greater number of interaction centers.[20,21] Previous studies have shown that not all particles should be treated as a macroscopic or a classical small hydrophobic object. For example, neopentane is too small to be treated as macroscopic, while fullerene and adamantane are too large to be considered as classical small objects but too small to be considered as macroscopic.[2,3]

The solubility of nonpolar molecules is determined by the balance of two factors: the excluded volume entropy change because of cavity formation in water and the direct solute−solvent van der Waals interactions. The first factor depends only on the solute size and leads to low solubility of nonpolar particles in water. However, solubility is also determined by the strength of the direct solute−solvent van der Waals interactions and induced dipole interactions. Some calculations were also conducted in vacuo, and it was confirmed that the potential of mean force (PMF) plot for nonpolar particles has a characteristic shape for Lennard−Jones-like interactions.[2,3,22]

It has been found that the solvent contribution to the PMF changes from negative for small molecules, through nearly zero for isobutane or neopentane, to positive for large molecules. The structure of water in the vicinity of nonpolar dimers was also analyzed. Weak ordered structure of the first hydration shell was observed. Hydrogen bonds involving the water molecules near the solute particles were smaller but stronger than those for bulk water.[2,3] Other studies were focused on temperature-dependent hydrophobic interactions. It was argued that these interactions could be entropy- or energy-driven. According to these studies, the hydrophobic interactions are entropy-driven for fullerene, while they are energy-driven for neopentane or adamantane.[5]

Generally, most of the studies on hydrophobicity are focused on PMFs for two nonpolar molecules in water,[23−27] their relationship with temperature[10,18,20,21,28−30] and pressure,[31−34] determination of thermodynamical properties of nonpolar particles,[35−37] and influence of cosolvents on hydrophobic interactions.[38]

It was concluded that the presence of NaCl precipitates methane because of unfavorable solute−solvent change of entropy.[39] Furthermore, fluctuations in the density of water molecules around the solute were intensively studied.[40]

There are only few studies on the influence of the ionic strength of the solution or on the salt effects on hydrophobic interactions.[41−44] It is well known that the solubility of nonpolar particles decreases in the presence of salts.[45] The following two types of ions are thought to exist: the "kosmotropes" and the "chaotropes." The kosmotropes enhance the hydrophobic effect by tightening the structure of water around the ions. Conversely, the chaotropes weaken this effect by disordering the structure of water around the ions. Because of these contrasting effects, the kosmotropes probably stabilize proteins and the chaotropes destabilize them. Two factors determine which ions belong to these groups, namely, the ionic charge and size.[46−51] For example, according to this theory, sodium chloride is a weak kosmotrope.[52] As affirmed later, this explanation was only an approximation. It should be noted that ions can have specific interactions with solutes.[53] The increasing magnitude of hydrophobic attraction between the methane molecules in the presence of salts and their decreased solubility was confirmed. Other studies have also focused on salt effects on methane solutions in water.[41,43,51,54] For methane dimers, the contribution of salts to the solvation free energy was enthalpic at low temperatures but became entropic at temperatures higher than 390 K.[51] In the presence of salts, the structure of water around the solute molecules was less ordered than that in pure water. It was found that although H-bonds are almost identical in water with salts, there is a large amount of broken H-bonds in the hydration shell of methane. An increase in free energy of the solution was also observed.[41,42]

The development of the theory of hydrophobicity has a long history. Initially, it was postulated that water molecules around a nonpolar molecule displace into an "iceberg," and this theory was then further elaborated.[55] It was then noted that the role of water molecules in attraction between nonpolar molecules is greater than direct van der Waals interactions between those particles. The existing models, which explained hydrophobic interactions based on entropic or enthalpic effects, consider charge fluctuations or dipole interactions. It is argued that short-range attraction is the only force between small hydrophobic surfaces and that multibody interactions are also important for large hydrophobic surfaces.[40,56,57] There are many models on the relationship between solute size and its shape and hydrophobic effects. Solute size and shape affect, for example, entropy, Gibbs hydration free energy, enthalpy, and finally, depth of the PMF.[3] It was found that PMF for large particles is less deep because of stronger solute−water interactions. Furthermore, it was confirmed that transfer of small solutes into water required large positive heat capacity, while no such large changes in heat capacity or entropy were required for transfer of large solutes.[17] A broader discussion on models was included in studies that focused on the relationships between hydrophobic theories.[1,3,57,58] Zangi et al. investigated the influence of different salts on hydrophobic interactions. They found that high-charge density ions strengthen the hydrophobic interactions between hydrophobic surfaces and low-charge density ions weaken these interactions.[59] In the present work, we focused only on the influence of sodium chloride, as an example of a simple salt, on hydrophobic interactions of nearly spherical and spheroidal particle dimers. Studies relevant to salt effect on macromolecular collapse such as protein folding or polymer collapse can be found in the literature.[60] The purpose of our study was to determine how the presence of the ions that are present at physiological conditions influences hydrophobic association. The ions that are predominant in body fluids are the chloride cations (approx. 142 mmol/dm^3) and sodium anions (approx. 103 mmol/dm^3). Next in abundance is the hydroxycarbonate anion with the content of 27 mmol/dm^3, followed by K^+ with 5 mmol/dm^3 content, while the other ions have 2.5 mmol/dm^3 or less content.[61] In view of this, restricting the study to NaCl solutions seems to be a reasonable choice. To the best of our knowledge, such type of studies present in this work have never been done before.

https://dx.doi.org/10.1021/acs.jpcb.0c06399
J. Phys. Chem. B 2020, 124, 10326−10336

Taken together, hydrophobic interactions and the presence of salts can significantly affect protein stability. This is especially important in protein structure predictions. Considering the influence of ionic strength on hydrophobicity can help in developing theoretical methods for protein structure predictions and for studying protein-folding processes, particularly, using the coarse-grained models.

In the present paper, we assess how the ionic strength, size, and shape of nonpolar molecules together affect hydrophobic interactions. The dimers of methane, neopentane, adamantane, fullerene, ethane, propane, butane, hexane, octane, and decane were simulated by umbrella sampling molecular dynamics (MD) in water under different conditions and ionic strength values. The PMFs of these dimers were determined, analyzed, and discussed.

METHODS

Series of umbrella sampling MD simulations were performed by sampling of the configurational space (necessary in the umbrella sampling method). Simulations were then performed for the hydrophobic dimers of methane, neopentane, adamantane, fullerene C_{60}, ethane, propane, butane, hexane, octane, and decane molecules. Each dimer was immersed in a periodic TIP3P[62] and for comparison in TIP4PEW[63] water boxes with sides around 60 and 59 Å, respectively. MD simulations were performed in two steps. The same procedures were used for both solvent models. First, each system was equilibrated under the *NPT* conditions (constant number of particles, constant pressure, and constant temperature) at T = 298 K and p = 1 atm for 500 ps. In the second step, the last configuration obtained in the first step was used as the starting point to conduct *NVT* ensemble simulations (constant number of particles, constant volume, and constant temperature) at T = 298 K for 5000 ps. The integration time step was 2 fs. For all nonbonded interactions, a 10 Å cutoff was used, and the electrostatic energy was estimated by the particle-mesh Ewald summation.[64] For all dimers, a series of 11 windows (15 windows for fullerene) of 5 ns simulation per window was run. Every window had a different harmonic restraint potential (eq 1) enforced on the distance (ξ) between two atoms (one from each molecule in dimer) that are closest to the center of the mass of each of the particle

$$V(\xi) = k(\xi - d_0)^2 \quad (1)$$

where k is the force constant (k = 2 kcal/mol/Å^2) and d_0 is the equilibrium distance for each pair (equals to 4.0, 5.0, 6.0, ..., 14.0 Å for all dimers for windows 1−11 and to 18 Å for fullerene for windows 1−15). The snapshots from MD simulations were saved every 0.2 ps. A total of 25,000 configurations were generated for each window.

The simulations were performed with the homodimer of nonpolar molecules and 7022 water molecules. Simulations with ions were also included and consisted of (1) dimer, 7012 water molecules, 5 Na^+, and 5 Cl^- ions; (2) dimer, 7002 water molecules, 10 Na^+, and 10 Cl^- ions; and (3) dimer, 6922 water molecules, 50 Na^+, and 50 Cl^- ions. This enabled us to study the influence of ionic strength on hydrophobic interactions. The ionic strength values were equal to 0.04, 0.08, and 0.40 mol/dm^3.

In our calculations, we assumed the charges on the atoms of solute molecules needed for AMBER 16.0[65] as zero. The AMBER atom types used in MD simulations were CT (denotes sp^3 aliphatic carbon atom) for all carbon atoms and HC (denotes hydrogen atom attached to the aliphatic carbon atom) for all hydrogen atoms.

To determine the PMF, the results from each window were processed using the weighted histogram analysis method (WHAM).[66,67] One-dimensional histograms (dependent only on the distance between the geometric centers of interacting particles) were plotted; thus, the histograms were averaged over all possible orientations. The calculated PMFs should tend to become 0 with increasing distance (after subtracting the constant factor accounting for the hydrophobic hydration free energy of the isolated solute molecule). The PMF baseline value was computed as the average of the PMF distance past 12 Å for neopentane, methane, and adamantane, past 11 Å for ethane, propane, butane, hexane, octane, and decane, and past 16 Å for fullerene.

Additionally, a sample plot was prepared to show the dependence of the PMF on the number of configurations collected from each window for adamantane dimer at the ionic strength of 0 mol/dm^3. Figure 1 shows that when the number of configurations increases, convergence is gained. The plots overlap in both TIP3P (Figure 1a) and TIP4PEW (Figure 1b) water models.

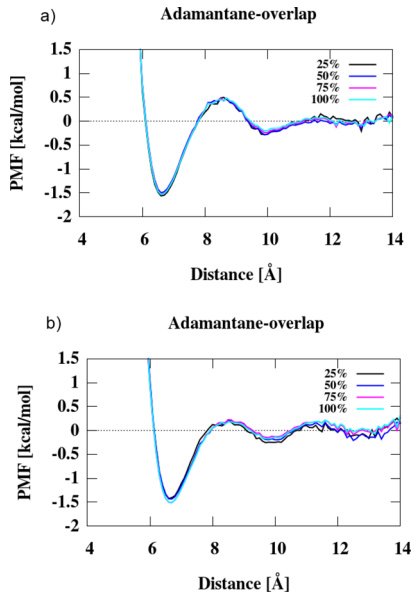

Figure 1. Overlap PMF of adamantane at ionic strength 0 mol/dm^3 for 6250 (25%), 12,500 (50%), 18,750 (75%), and 25,000 (100%) configurations in (a) TIP3P and (b) TIP4PEW water models.

We also assayed water structure in the proximity of solute molecules. For PMF calculations, only cartesian coordinates of the solute were stored in our MD simulations. Therefore, to determine the density and number of hydrogen bonds of water molecules near the solutes, additional 5 ns simulations were performed for adamantane and hexane in both TIP3P and TIP4PEW water models (cartesian coordinates of all atoms were stored every 0.2 ps this time). To keep monomers at distances of contact minima and solvent-separated minima, harmonic restraints were enforced. The positions of contact minima and solvent-separated minima were as follows: for adamantane, 6.6, 10.0 Å at IS = 0 mol/dm^3 and 6.6, 10.1 Å at IS = 0.40 mol/dm^3 in the TIP3P water model and 6.7, 9.8 Å at IS = 0 mol/dm^3 and 6.7, 9.7 Å at IS = 0.40 mol/dm^3 in the

https://dx.doi.org/10.1021/acs.jpcb.0c06399
J. Phys. Chem. B 2020, 124, 10326−10336

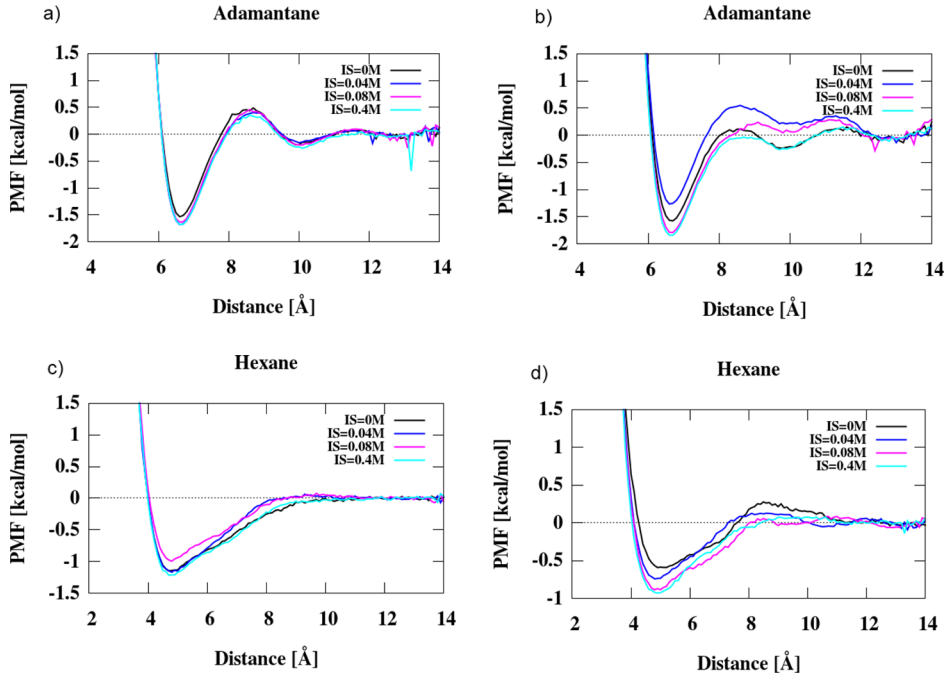

Figure 2. PMFs at different ionic strength values for adamantane dimer in (a) TIP3P and (b) TIP4PEW water models and for hexane dimer in (c) TIP3P and (d) TIP4PEW water models.

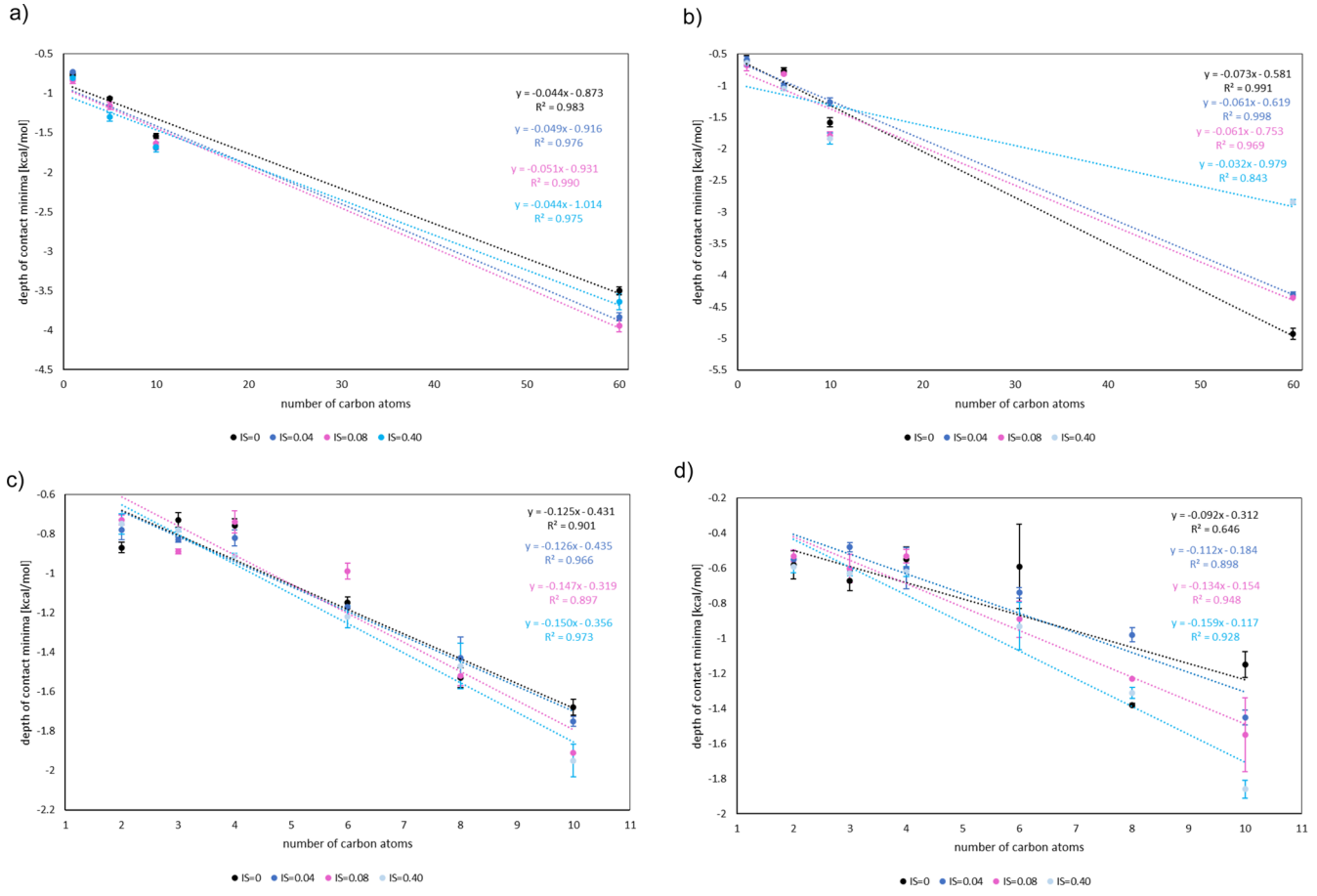

Figure 3. Dependence of depth of contact minima (with standard deviations as error bars) in PMF at different values of ionic strength on the number of carbon atoms in spherical molecules in (a) TIP3P and (b) TIP4PEW water models and for spheroidal molecules in (c) TIP3P and (d) TIP4PEW water models.

https://dx.doi.org/10.1021/acs.jpcb.0c06399
J. Phys. Chem. B 2020, 124, 10326−10336

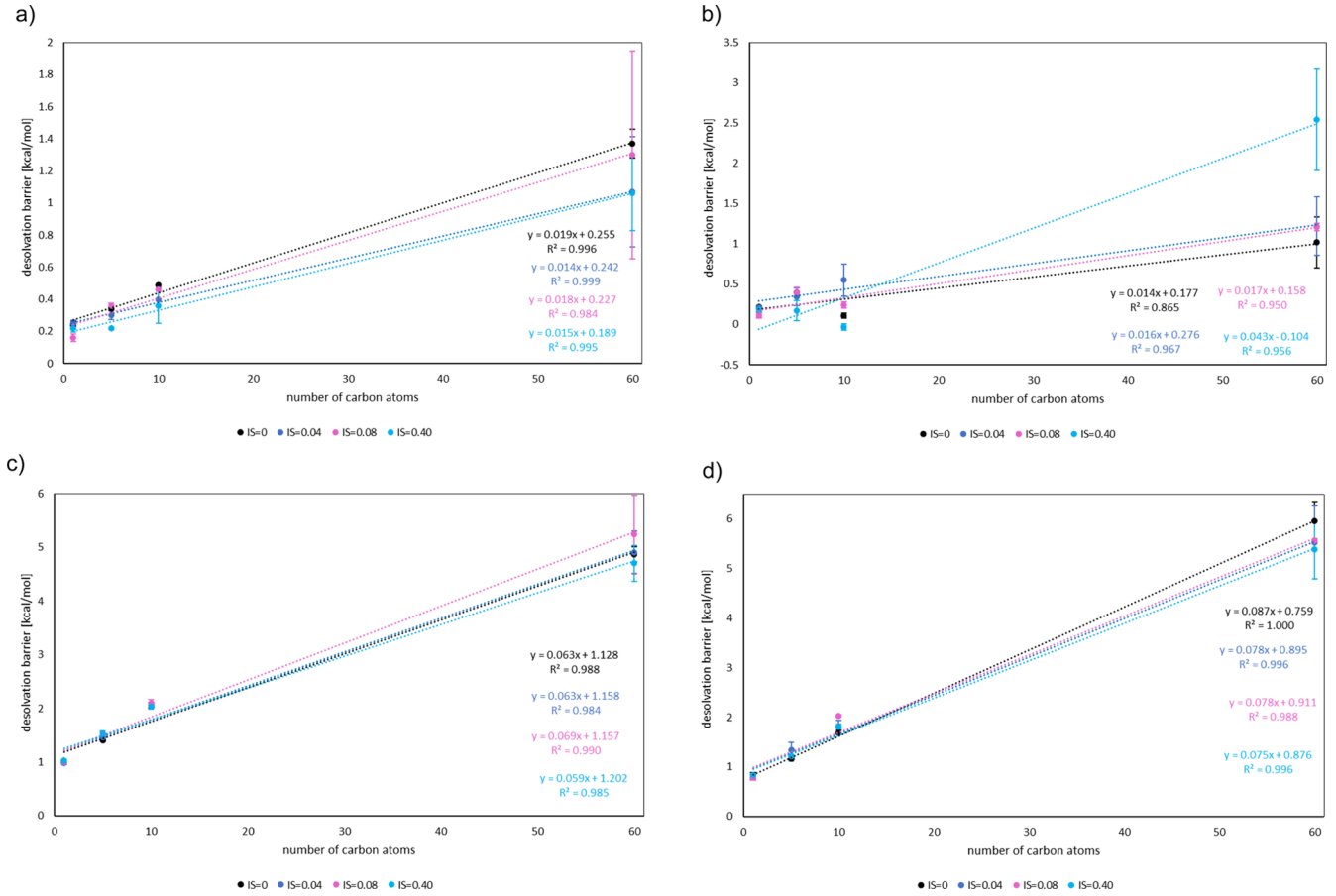

Figure 4. Dependence of desolvation energy barrier (with standard deviations as error bars) calculated as a height of desolvation maximum (counting from baseline $y = 0$) on the number of carbon atoms in spherical molecules in (a) TIP3P and (b) TIP4PEW water models and calculated as difference between the CM depth and the height of desolvation maximum on the number of carbon atoms in spherical molecules in (c) TIP3P and (d) TIP4PEW water models.

TIP4PEW model; for hexane, 4.8, 7.8 Å at IS = 0 mol/dm^3 and 4.7, 7.7 Å at IS = 0.40 mol/dm^3 in the TIP3P water model and 4.9, 7.9 Å in the TIP4PEW model for both ionic strength values. All distributions were expressed in cylindrical coordinates **h** (passing through the line connecting the centers of the solute molecules) and **r** (perpendicular to axis **h**) and were averaged over the azimuthal angle. We computed the distribution over all points of the two-dimensional grid in **h** and **r** of water molecule density and the average number of hydrogen bonds between water particles (based on oxygen−oxygen distance not greater than 3.5 Å and H−O···O angle smaller than 30°). Two-dimensional maps for all distributions were prepared with 0.2 Å grid. Technical details can be found elsewhere.[2,3,68]

RESULTS AND DISCUSSION

PMF. Figure 2 shows the results of calculations of the PMF at different ionic strength values for adamantane dimer in the TIP3P (a) and TIP4PEW (b) water models and for hexane dimer in the TIP3P (c) and TIP4PEW (d) water models using the umbrella sampling/WHAM method. PMF plots for methane, neopentane, fullerene, ethane, propane, butane, octane, and decane dimers are included in the Supporting Information (Figures S1−S8).

For most of the compounds, PMF plots exhibited characteristic shapes with two minima and one maximum. The first minimum, the deepest one, is referred to as the contact minimum (CM). It occurs at approximately 3.9, 5.8, 6.6, 10.0, 4.5, 5.0, 5.1, 4.8, 4.9, and 4.7 Å corresponding to methane, neopentane, adamantane, fullerene, ethane, propane, butane, hexane, octane, and decane, respectively, in the TIP3P water model. In the TIP4PEW model, the situation is similar, and the positions of minima are the same or slightly shifted by approximately 0.1−0.2 Å. In both solvent models, the position of CM changes slightly when the ionic strength varies. The deepest CM for nearly spherical particles is observed for fullerene with a depth of around −3.5 to −3.94 kcal/mol depending on the ionic strength value in the TIP3P model and −2.84 to −4.93 kcal/mol in the TIP4PEW model (Figure S3). For ethane, propane, and butane, the depth of CM in the TIP3P model is similar and is around −0.7 to −1.0 kcal/mol depending on the ionic strength value (Figures S4−S6), and for longer hydrocarbons, that is, hexane, octane, and decane, the average depth of CM is −1.1, −1.5, and −1.8 kcal/mol, respectively (Figures 2c,f, S7 and S8). In TIP4PEW, CM is shallower than that in TIP3P (under the same ionic strength conditions) for each spherical (methane, neopentane, adamantane, and fullerene) and spheroidal (ethane, propane, butane, hexane, octane, and decane) compound.

The second minimum corresponds to distances at which one water molecule enters the space between two interacting particles and is called solvent-separated minimum (SSM). In the TIP3P model, SSMs occur at distances of 7.3, 9.2, 10.0, 13.6, 7.8, 8.7, and 9.2 Å for methane, neopentane, adamantane,

https://dx.doi.org/10.1021/acs.jpcb.0c06399
J. Phys. Chem. B 2020, 124, 10326−10336

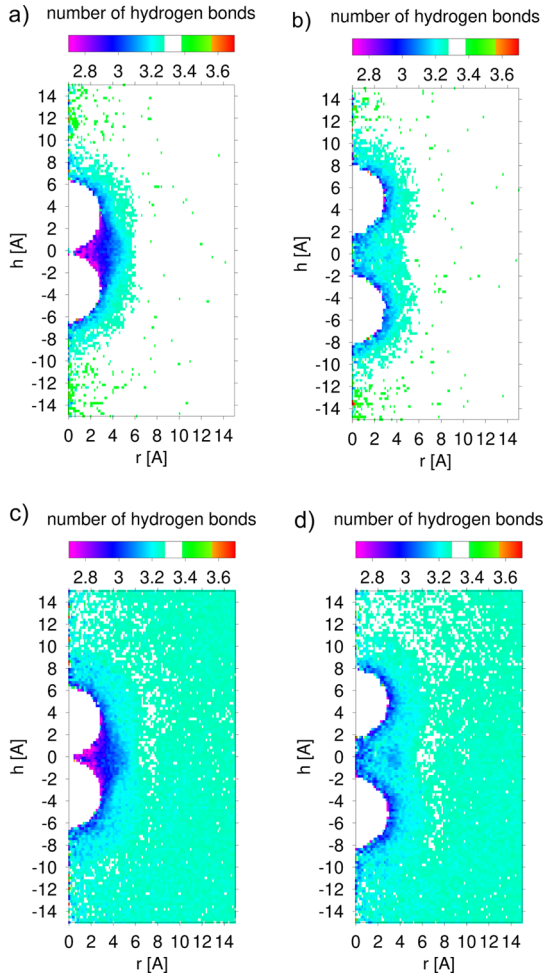

Figure 5. Distribution of average number of hydrogen bonds between water molecules in the vicinity of adamantane dimer at IS = 0 mol/dm^3 at distances between solute particles of (a) 6.6 Å (CM) and (b) 10.0 Å (SSM) and at IS = 0.40 mol/dm^3 at distances between solute particles (c) 6.6 Å (CM) and (d) 10.1 Å (SSM) in TIP3P water model. The color scale is shown above the maps, and the average number of H-bonds for bulk water is displayed as white.

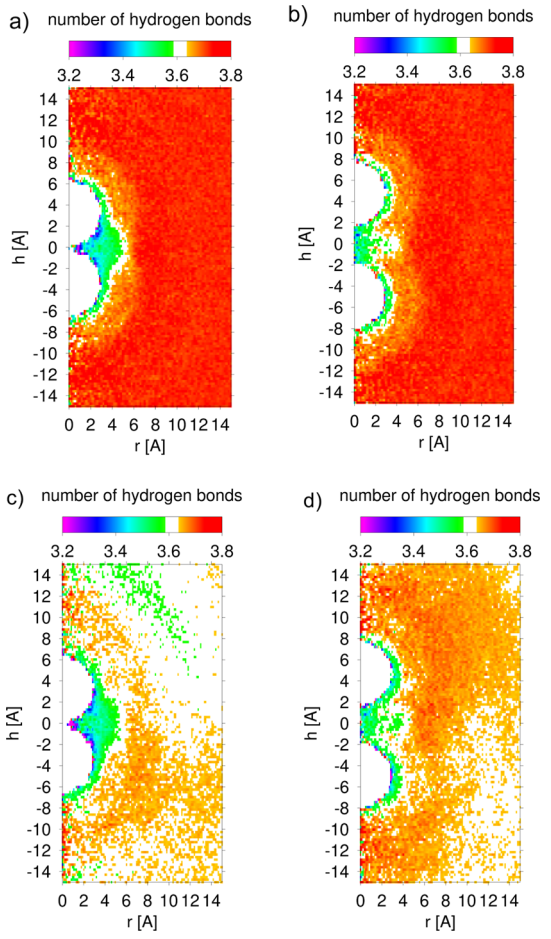

Figure 6. Distribution of average number of hydrogen bonds between water molecules in the vicinity of adamantane dimer at IS = 0 mol/dm^3 at distances between solute particles of (a) 6.7 Å (CM) and (b) 9.8 Å (SSM) and at IS = 0.40 mol/dm^3 at distances between solute particles of (c) 6.7 Å (CM) and (d) 9.7 Å (SSM) in TIP4PEW water model. The color scale is shown above the maps, and the average number of H-bonds for bulk water is displayed as white.

fullerene, ethane, propane, and butane, respectively. These positions differ maximally by 0.3 Å depending on the ionic strength value. For hexane, octane, and decane, it is difficult to define SSM precisely (Figures 2c,d, S7 and S8). In the TIP4PEW water model, the positions of SSMs differ from those in TIP3P by around 0.1−0.3 Å. Interestingly, for fullerene, it is difficult to define the position of SSM in the TIP4PEW model compared to that in the TIP3P model. In the PMF of butane in the TIP4PEW model, SSM can be defined at IS = 0, 0.04 and 0.08 mol/dm^3. In contrast, there are difficulties to precisely define SSM at IS = 0.40 mol/dm^3. For hexane, octane, and decane, the situation is the same as that in the TIP3P water model, that is, SSMs could not be defined.

The third characteristic feature of the PMF plot is the maximum located between CM and SSM. It corresponds to desolvation maximum. This maximum is observed for most of the investigated dimers and occurs in the TIP3P model at distances of 5.8, 7.9, 8.7, 12.0, 6.4, 6.9, and 7.6 Å for methane, neopentane, adamantane, fullerene, ethane, propane, and butane, respectively. As noted earlier, the maximum positions differ according to the ionic strength value. For hexane, octane, and decane, the situation is similar to that observed for SSM, that is, it is difficult to define the maximum. As observed for CM and SSM, the position of desolvation maximum in TIP4PEW differs slightly from that in TIP3P. CM, SSM, and desolvation maximum are shifted to longer distances when the size of nearly spherical particles increases, and the depths of these extrema become deeper. This finding has also been confirmed in previous studies.[2,3,5] In the PMF plots of spherical particles (methane, neopentane, adamantane, and fullerene), the influence of ionic strength was observed. When sodium and chloride ions are present in water, CM depths increase in every case. The situation is the same in the TIP4PEW water model for smaller particles (methane and neopentane), but for fullerene and adamantane, the PMF plots are more indented [Figure 3 in TIP3P (a) and TIP4PEW (b) water models, respectively]. Figure 3a,b shows the dependence of CM depth on the number of carbon atoms in models of spherical particles at different ionic strength values. The findings confirmed a tendency to deepen CM in the presence of salts in solution in the TIP3P water model. It was concluded that with the increase in ionic strength, there is greater tendency of hydrophobic interactions between those dimers than the existence of two isolated monomers. This implies that hydrophobic interactions are stronger. The situation is slightly

https://dx.doi.org/10.1021/acs.jpcb.0c06399
J. Phys. Chem. B 2020, 124, 10326−10336

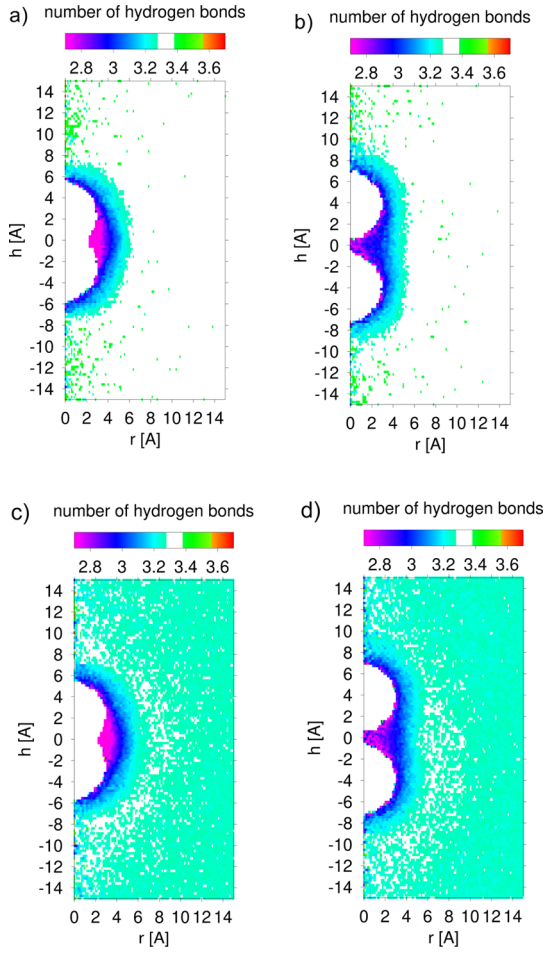

Figure 7. Distribution of average number of hydrogen bonds between water molecules in the vicinity of hexane dimer at IS = 0 mol/dm^3 at distances between solute particles of (a) 4.8 Å (CM) and (b) 7.8 Å (SSM) and at IS = 0.40 mol/dm^3 at distances between solute particles of (c) 4.7 Å (CM) and (d) 7.7 Å (SSM) in TIP3P water model. The color scale is shown above the maps, and the average number of H-bonds for bulk water is displayed as white.

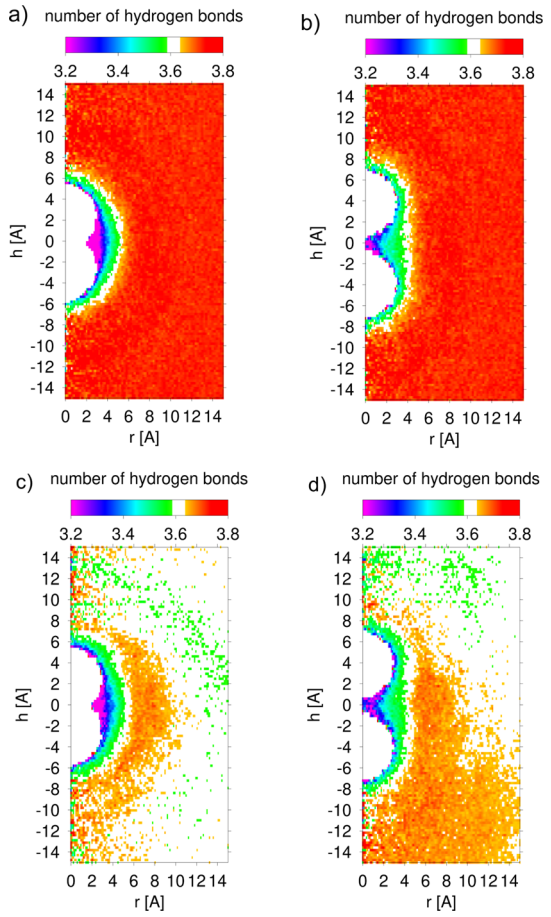

Figure 8. Distribution of average number of hydrogen bonds between water molecules in the vicinity of hexane dimer at IS = 0 mol/dm^3 at distances between solute particles of (a) 4.9 Å (CM) and (b) 7.9 Å (SSM) and at IS = 0.40 mol/dm^3 at distances between solute particles of (c) 4.9 Å (CM) and (d) 7.9 Å (SSM) in TIP4PEW water model. The color scale is shown above the maps, and the average number of H-bonds for bulk water is displayed as white.

different in the TIP4PEW model. The slope of correlation decreases for nearly spherical particles. However, this correlation is grounded mostly on the difference between fullerene and the remaining particles. The slope of correlation increases (in absolute value) with the increase in the ionic strength value after excluding fullerene from the statistics, with the exception of IS = 0.04 M (Figure S9). It is worth noting that fullerene is much larger in size than the remaining studied compounds. It was also previously proven that fullerene cannot be treated as a classical hydrophobic particle.[2]

The depth of SSM mostly increases when salts are present in solution, especially at the highest value of ionic strength. Generally, the heights of desolvation maxima become lower when the ionic strength values increase. The only exception is fullerene, where changes of desolvation maxima are within error bars. However, as we mentioned before, fullerene is a much bigger particle than the remaining compounds considered in this work and cannot be treated as a classical hydrophobic one. Desolvation energy barriers could be defined as heights of desolvation maxima (counting from baseline y = 0). It was observed that the barrier decreases when salts are present in solution (Figure 4a) (again with exception of fullerene). The largest decline is observed when the ionic strength value is greater than the physiological one and is equal to 0.40 mol/dm^3. The second approach to desolvation energy barrier assumed that this barrier is calculated as the difference between the CM depth and the height of desolvation maximum. In our case, this analysis showed that for smaller molecules, such as methane, adamantane, and neopentane, changes in barrier were not so significant as those for fullerene (Figure 4c). It was observed that barriers differed slightly or were comparable at different ionic strength values for methane and adamantane. For neopentane, the barrier was higher with the increase in ionic strength. However, for fullerene, the barrier first increases, and at IS = 0.40 mol/dm^3, it decreases to a value lower than that at IS = 0 mol/dm^3; this further confirms that fullerene cannot be treated as a classical hydrophobic molecule.[2]

In the TIP4PEW water model, the desolvation energy barrier, counting from baseline y = 0, increases with the increase in ionic strength (Figure 4b), but the barrier defined as the difference between the CM depth and the desolvation maximum height decreases (Figure 4d).

For spheroidal-shaped compounds (ethane, propane, butane, hexane, octane, and decane), the PMF plots are slightly deformed. CM is well observed, but SSM and

https://dx.doi.org/10.1021/acs.jpcb.0c06399
J. Phys. Chem. B 2020, 124, 10326−10336

desolvation maxima are not so broad. They become more unclear with the increase in the length of carbon chain, regardless of the ionic strength of solution in both water models. This is presumably caused by the computational assumption, that is, PMFs were averaged over all orientations. However, such assumption does not affect the results for nonpolar particles.[69]

Higher ionic strength values and changes in the length of carbon chain of interacting particles result mostly in deeper CM (Figure 3c,d). This shows stronger hydrophobic interactions in the presence of salts, which is consistent with nearly spherical molecules. The situation is opposite only for ethane and octane. Changes at IS = 0.08 mol/dm^3 are unpredictable and differ from those observed at other ionic strength values. The situation is similar for the TIP4PEW model, wherein the slope of correlation increases with the increase in ionic strength (from 0.092 at IS = 0 mol/dm^3 to 0.159 at IS = 0.40 mol/dm^3).

Figure for the relationship between the desolvation barrier and the number of carbon atoms for spheroidal molecules cannot be created because PMF plots were deformed for longer hydrocarbons, as mentioned earlier.

It is worth noting that in the PMF plots from the TIP4PEW water model, we noted the presence of the second maximum after SSM. It is visible in the PMF plots of methane, neopentane, adamantane, ethane, propane, and butane.

Distribution of Water Molecule Density and Hydrogen Bonds. Two-dimensional distribution functions describing water density and average number of hydrogen bonds between water molecules were calculated.

Figures S10−S13 show the two-dimensional maps of the normalized distribution function of water density around adamantane (represents spherical particles) and hexane (represents spheroidal particles) dimers at two selected distances between the center of molecules (for adamantane, 6.6, 10.0 Å at IS = 0 mol/dm^3 and 6.6, 10.1 Å at IS = 0.40 mol/dm^3 in the TIP3P water model and 6.7, 9.8 Å at IS = 0 mol/dm^3 and 6.7, 9.7 Å at IS = 0.40 mol/dm^3 in the TIP4PEW model; for hexane, 4.8, 7.8 Å at IS = 0 mol/dm^3 and 4.7, 7.7 Å at IS = 0.40 mol/dm^3 in the TIP3P water model and 4.9, 7.9 Å in the TIP4PEW model for both ionic strength values) which correspond to the positions of CM and SSM. SSM for hexane dimer was imposed by adding 3 Å to the CM distance [because of the size (diameter) of water particle entering the space between dimer plus some additional space]. The first solvation sphere for adamantane has lower density than that for bulk water at both ionic strengths, 0 and 0.40 mol/dm^3, in the TIP3P water model. There is quite a large space in contact with the solute particles in which the density of water is lower than 0.5. A similar situation was observed in the water density map for hexane (Figures S12 and S13). In the TIP4PEW model (Figures S11 and S13), large differences compared to the TIP3P model (Figures S10 and S12) cannot be observed. On the basis of these maps (Figures S10−S13), it can be concluded that solutes experienced water-mediated repulsive interactions, which was confirmed in the studies of Ben-Amotz.[70]

Figures 5−8 show the cylindrical distribution of the average number of hydrogen bonds between water molecules around adamantane (Figures 5 and 6) and hexane (Figures 7 and 8) dimers. In the TIP3P model (Figures 5 and 7), the average number of H-bonds between water molecules in the solvation sphere of adamantane dimer is lower than that in bulk water. Moreover, the number of broken hydrogen bonds in the space between solute molecules is much greater than that in bulk water. This is particularly visible in the map corresponding to the CM of adamantane. At IS = 0.40 mol/dm^3, some differences were observed. The number of H-bonds is also slightly lower than that in bulk water at longer distances from solute molecules. It was also observed that for maps corresponding to SSM, the number of H-bonds in the space between solute particles is lower than that in bulk water at broader space than at IS = 0 mol/dm^3. For the hexane dimer, similar relationships as those for adamantane are observed at both IS = 0 and 0.40 mol/dm^3. However, more broken H-bonds in the space between dimers are observed in the hexane dimer than in the adamantane dimer. This is due to the spherical shape of adamantane and the spheroidal shape of hexane.

The situation is quite different in the TIP4PEW water model (Figures 6 and 8). In the vicinity of solutes, the number of hydrogen bonds between water molecules is still lower than that in bulk water, but it increases with the distance from the vicinity. This relationship was observed for both adamantane and hexane at IS = 0 mol/dm^3. At IS = 0.40 mol/dm^3, the number of H-bonds around solute molecules does not change, but at longer distances from solute particles, there are more broken hydrogen bonds than that observed at lower ionic strength values. Moreover, the structure of water (particles further from solute) at IS = 0.40 mol/dm^3 changes as the distance between dimers increases. More H-bonds appear at the distance corresponding to SSM.

CONCLUSIONS

PMF plots of 10 homodimers of nonpolar particles, namely, methane, neopentane, adamantane, fullerene, ethane, propane, butane, hexane, octane, and decane, in two water models (TIP3P and TIP4PEW) were determined. Most of the PMF plots showed a characteristic shape for hydrophobic interactions with CM, SSM, and desolvation maxima. PMF plots were deformed for longer hydrocarbons.

It was observed that when the ionic strength increases, the slope of correlation between the CM depth and the number of carbon atoms also increases, although with some exceptions. The same tendency was observed for spherical and spheroidal particles. Furthermore, it was confirmed that for larger particles, CM becomes deeper and their positions are shifted toward longer distances.

Both the salting-out effect and constants (so-called Setschenow constants)[71] determine the correlation between the presence of salts in aqueous solution, solubility and properties of organic compounds. Organic compounds such as organic acids, aromatic and alkane hydrocarbons, and their chloro-derivative are less soluble in electrolyte solutions then in pure water. This phenomenon is correlated with molar volumes of organic compounds and is greater for high concentration. The salting-out constants obtained for sea water (natural and synthetic) and the solution of NaCl point out similar salting-out properties (at the same concentration level). Moreover, based on these results, the sea water salting-out factor, described by the function of organic compounds molar volume, was suggested. The reduction of organic solute solubility is equal to 1.36.[71,72] The same general tendency is observed for our group of compounds: increasing the depth of CM according to the increase of ionic strength values.

https://dx.doi.org/10.1021/acs.jpcb.0c06399
J. Phys. Chem. B 2020, 124, 10326−10336

Comparison between two water models, TIP3P and TIP4PEW, shows that the TIP3P model mostly enables calculations with higher or similar correlation coefficient R^2 to the TIP4PEW model. According to the literature, the TIP4PEW water model (which is more advanced than TIP3P) is more precise in predicting properties of bulk water but less accurate in projecting hydration energies of small particles than TIP3P.[73−75] Our results showed that the hydration properties of water were sensitive to the choice of water model. The choice of solvent model has a greater effect on the unfolded state than on the folded state of peptides,[76] which is crucial in such studies. Experimental data could be helpful in deciding which model is more reliable for hydrophobic interactions; however, such data are currently unavailable. In our opinion (based on the obtained results), the TIP3P model seems to be more suitable for such type of studies.

On the basis of two-dimensional distribution functions describing water density and average number of hydrogen bonds between water molecules, it was observed that the increase in ionic strength does not change the water density but changes the average number of H-bonds.

■ ASSOCIATED CONTENT

Supporting Information

The Supporting Information is available free of charge at https://pubs.acs.org/doi/10.1021/acs.jpcb.0c06399.

PMFs calculated in TIP3P and TIP4EW water models for homodimers of methane, neopentane, fullerene, ethane, propane, butane, octane, and decane; dependence of depth of contact minima (with standard deviations as error bars) in PMF at different values of ionic strength on the number of carbon atoms in nearly spherical molecules without fullerene molecule; and normalized distribution functions of water density in the vicinity of adamantane and hexane dimer at IS = 0 mol/dm^3 and IS = 0.40 mol/dm^3 in both TIP3P and TIP4PEW water models (PDF)

■ AUTHOR INFORMATION

Corresponding Author

Mariusz Makowski − *Faculty of Chemistry, University of Gdańsk, 80-308 Gdańsk, Poland;* orcid.org/0000-0002-7342-722X; Email: mariusz.makowski@ug.edu.pl

Author

Małgorzata Bogunia − *Faculty of Chemistry, University of Gdańsk, 80-308 Gdańsk, Poland*

Complete contact information is available at: https://pubs.acs.org/10.1021/acs.jpcb.0c06399

Notes

The authors declare no competing financial interest.

■ ACKNOWLEDGMENTS

This work was supported by grants from the Polish National Science Centre (UMO-2013/10/E/ST4/00755), BMN 539-T120-B468-20 from Polish Ministry of Science and Higher Education, and WND-POWR.03.02.00-00-I059/16 from The National Centre for Research and Development. Calculations were conducted by using the resources of cluster PIASEK at the Faculty of Chemistry, University of Gdansk.

■ REFERENCES

(1) Scheraga, H. A. Theory of Hydrophobic Interactions. *J. Biomol. Struct. Dyn.* **1998**, *16*, 447−460.

(2) Makowski, M.; Czaplewski, C.; Liwo, A.; Scheraga, H. A. Potential of Mean Force of Association of Large Hydrophobic Particles: Toward the Nanoscale Limit. *J. Phys. Chem. B* **2010**, *114*, 993−1003.

(3) Sobolewski, E.; Makowski, M.; Czaplewski, C.; Liwo, A.; Ołdziej, S.; Scheraga, H. A. Potential of Mean Force of Hydrophobic Association: Dependence on Solute Size. *J. Phys. Chem. B* **2007**, *111*, 10765−10774.

(4) Blokzijl, W.; Engberts, J. B. F. N. Hydrophobic Effects. Opinions and Facts. *Angew. Chem., Int. Ed.* **1993**, *32*, 1545−1579.

(5) Bartosik, A.; Wiśniewska, M.; Makowski, M. Potentials of Mean Force for Hydrophobic Interactions between Hydrocarbons in Water Solution: Dependence on Temperature, Solute Shape, and Solute Size. *J. Phys. Org. Chem.* **2015**, *28*, 10−16.

(6) Tanaka, S.; Scheraga, H. A. Hypothesis about the Mechanism of Protein Folding1. *Macromolecules* **1977**, *10*, 291−304.

(7) Matheson, R. R.; Scheraga, H. A. A Method for Predicting Nucleation Sites for Protein Folding Based on Hydrophobic Contacts. *Macromolecules* **1978**, *11*, 819−829.

(8) Nemethy, G.; Scheraga, H. A. A Possible Folding Pathway of Bovine Pancreatic RNase. *Proc. Natl. Acad. Sci. U.S.A.* **1979**, *76*, 6050−6054.

(9) Ben-Naim, A. Solvent-Induced Interactions: Hydrophobic and Hydrophilic Phenomena. *J. Chem. Phys.* **1989**, *90*, 7412−7425.

(10) Griffith, J. H.; Scheraga, H. A. Statistical Thermodynamics of Aqueous Solutions . I. Water Structure , Solutions with Non-Polar Solutes, and Hydrophobic Interactions. *J. Mol. Struct.: THEOCHEM* **2004**, *682*, 97−113.

(11) Hura, G.; Russo, D.; Glaeser, R. M.; Head-Gordon, T.; Krack, M.; Parrinello, M. Water Structure as a Function of Temperature from X-Ray Scattering Experiments and Ab Initio Molecular Dynamics. *Phys. Chem. Chem. Phys.* **2003**, *5*, 1981−1991.

(12) Turner, J.; Soper, A. K. The Effect of Apolar Solutes on Water Structure: Alcohols and Tetraalkylammonium Ions. *J. Chem. Phys.* **1994**, *101*, 6116−6125.

(13) Broadbent, R. D.; Neilson, G. W. The Interatomic Structure of Argon in Water. *J. Chem. Phys.* **1994**, *100*, 7543−7547.

(14) De Jong, B. P. H. K.; Wilson, J. E.; Neilson, G. W.; Buckingham, A. D. Hydrophobic Hydration of Methane. *Mol. Phys.* **1997**, *91*, 99−104.

(15) Rigby, M.; Prausnitz, J. M. Solubility of Water in Compressed Nitrogen, Argon, and Methane. *J. Phys. Chem.* **1968**, *72*, 330−334.

(16) Abdulagatov, I. M.; Bazaev, A. R.; Ramazanova, A. E. Volumetric Properties and Virial Coefficients of (Water+methane). *J. Chem. Thermodyn.* **1993**, *25*, 249−259.

(17) Southall, N. T.; Dill, K. A. The Mechanism of Hydrophobic Solvation Depends on Solute Radius. *J. Phys. Chem. B* **2000**, *104*, 1326−1331.

(18) Némethy, G.; Scheraga, H. A. The Structure of Water and Hydrophobic Bonding in Proteins. III. The Thermodynamic Properties of Hydrophobic Bonds in Proteins. *J. Phys. Chem.* **1962**, *66*, 1773−1789.

(19) Némethy, G.; Scheraga, H. A. Structure of Water and Hydrophobic Bonding in Proteins. II. Model for the Thermodynamic Properties of Aqueous Solutions of Hydrocarbons. *J. Chem. Phys.* **1962**, *36*, 3401−3417.

(20) Lüdemann, S.; Abseher, R.; Schreiber, H.; Steinhauser, O. The Temperature-Dependence of Hydrophobic Association in Water. Pair versus Bulk Hydrophobic Interactions. *J. Am. Chem. Soc.* **1997**, *119*, 4206−4213.

(21) Lüdemann, S.; Schreiber, H.; Abseher, R.; Steinhauser, O.; Schreiber, H.; Abseher, R.; Steinhauser, O.; Lu, S. The Influence of Temperature on Pairwise Hydrophobic Interactions of Methanelike Particles: A Molecular Dynamics Study of Free Energy The Influence of Temperature on Pairwise Hydrophobic Interactions of Methane-

like Particles: A Molecular Dynamics Study. *J. Phys. Chem.* **1996**, *104*, 286−295.
(22) Graziano, G. On the Size Dependence of Hydrophobic Hydration. *J. Chem. Soc., Faraday Trans.* **1998**, *94*, 3345−3352.
(23) Owicki, J. C.; Scheraga, H. A. Monte Carlo Calculations in the Isothermal-Isobaric Ensemble. 2. Dilute Aqueous Solution of Methane. *J. Am. Chem. Soc.* **1977**, *99*, 7413−7418.
(24) Rapaport, D. C.; Scheraga, H. A. Hydration of Inert Solutes. A Molecular Dynamics Study. *J. Phys. Chem.* **1982**, *86*, 873−880.
(25) Smith, D. E.; Haymet, A. D. J. Free Energy, Entropy, and Internal Energy of Hydrophobic Interactions: Computer Simulations. *J. Chem. Phys.* **1993**, *98*, 6445−6454.
(26) van Belle, D.; Wodak, S. J. Molecular Dynamics Study of Methane Hydration and Methane Association in a Polarizable Water Phase. *J. Am. Chem. Soc.* **1993**, *115*, 647−652.
(27) Young, W. S.; Brooks III, C. L. A Reexamination of the Hydrophobic Effect: Exploring the Role of the Solvent Model in Computing the Methane-Methane Potential of Mean Force. *J. Chem. Phys.* **1997**, *106*, 9265−9269.
(28) Chau, P.-L.; Mancera, R. L. Computer Simulation of the Structural Effect of Pressure on the Hydrophobic Hydration of Methane. *Mol. Phys.* **1999**, *96*, 109−122.
(29) Shimizu, S.; Chan, H. S. Temperature Dependence of Hydrophobic Interactions: A Mean Force Perspective, Effects of Water Density, and Nonadditivity of Thermodynamic Signatures. *J. Chem. Phys.* **2000**, *113*, 4683−4700.
(30) Ghosh, T.; García, A. E.; Garde, S. Molecular Dynamics Simulations of Pressure Effects on Hydrophobic Interactions. *J. Am. Chem. Soc.* **2001**, *123*, 10997−11003.
(31) Ghosh, T.; García, A. E.; Garde, S. Enthalpy and Entropy Contributions to the Pressure Dependence of Hydrophobic Interactions. *J. Chem. Phys.* **2002**, *116*, 2480−2486.
(32) Paschek, D. Temperature Dependence of the Hydrophobic Hydration and Interaction of Simple Solutes: An Examination of Five Popular Water Models. *J. Chem. Phys.* **2004**, *120*, 6674−6690.
(33) Paschek, D. Heat Capacity Effects Associated with the Hydrophobic Hydration and Interaction of Simple Solutes: A Detailed Structural and Energetical Analysis Based on Molecular Dynamics Simulations. *J. Chem. Phys.* **2004**, *120*, 10605−10617.
(34) Dias, C. L.; Chan, H. S. Pressure-Dependent Properties of Elementary Hydrophobic Interactions: Ramifications for Activation Properties of Protein Folding. *J. Phys. Chem. B* **2014**, *118*, 7488−7509.
(35) Islam, N.; Flint, M.; Rick, S. W. Water hydrogen degrees of freedom and the hydrophobic effect. *J. Chem. Phys.* **2019**, *150*, 014502.
(36) Cerdeiriña, C. A.; Debenedetti, P. G. Water's Thermal Pressure Drives the Temperature Dependence of Hydrophobic Hydration. *J. Phys. Chem. B* **2018**, *122*, 3620−3625.
(37) Pratt, L. R.; Chaudhari, M. I.; Rempe, S. B. Statistical Analyses of Hydrophobic Interactions: A Mini-Review. *J. Phys. Chem. B* **2016**, *120*, 6455−6460.
(38) van der Vegt, N. F. A.; Nayar, D. The Hydrophobic Effect and the Role of Cosolvents. *J. Phys. Chem. B* **2017**, *121*, 9986−9998.
(39) van der Vegt, N. F. A.; van Gunsteren, W. F. Entropic Contributions in Cosolvent Binding to Hydrophobic Solutes in Water. *J. Phys. Chem. B* **2004**, *108*, 1056−1064.
(40) Patel, A. J.; Varilly, P.; Chandler, D. Fluctuations of Water near Extended Hydrophobic and Hydrophilic Surfaces. *J. Phys. Chem. B* **2010**, *114*, 1622−1637.
(41) Mancera, R. L. Computer Simulation of the effect of Salt on the Hydrophobic effect. *J. Chem. Soc., Faraday Trans.* **1998**, *94*, 3549−3559.
(42) Mancera, R. L. Does Salt Increase the Magnitude of the Hydrophobic Effect? A Computer Simulation Study. *Chem. Phys. Lett.* **1998**, *296*, 459−465.
(43) Graziano, G. Role of Salts on the Strength of Pairwise Hydrophobic Interaction. *Chem. Phys. Lett.* **2009**, *483*, 67−71.
(44) Ghosh, T.; Kalra, A.; Garde, S. On the Salt-Induced Stabilization of Pair and Many-body Hydrophobic Interactions. *J. Phys. Chem. B* **2005**, *109*, 642−651.
(45) Tanford, C. *The Hydrophobic Effect: Formation of Micelles and Biological Membranes*; Wiley: New York, 1973.
(46) Franks, F. Protein Stability: The Value of Old Literature. *Biophys. Chem.* **2002**, *96*, 117−127.
(47) Hribar, B.; Southall, N. T.; Vlachy, V.; Dill, K. A. How Ions Affect the Structure of Water. *J. Am. Chem. Soc.* **2002**, *124*, 12302−12311.
(48) Collins, K. D.; Washabaugh, M. W. The Hofmeister Effect and the Behaviour of Water at Interfaces. *Q. Rev. Biophys.* **1985**, *18*, 323−422.
(49) Baldwin, R. L. How Hofmeister Ion Interactions Affect Protein Stability. *Biophys. J.* **1996**, *71*, 2056−2063.
(50) Dill, K. A.; Truskett, T. M.; Vlachy, V.; Hribar-Lee, B. Modeling Water, the Hydrophobic Effect, and Ion Solvation. *Annu. Rev. Biophys. Biomol. Struct.* **2005**, *34*, 173−199.
(51) Holzmann, J.; Ludwig, R.; Geiger, A.; Paschek, D. Temperature and Concentration Effects on the Solvophobic Solvation of Methane in Aqueous Salt Solutions. *ChemPhysChem* **2008**, *9*, 2722−2730.
(52) Collins, K. D. Charge Density-Dependent Strength of Hydration and Biological Structure. *Biophys. J.* **1997**, *72*, 65−76.
(53) Okur, H. I.; Hladílková, J.; Rembert, K. B.; Cho, Y.; Heyda, J.; Dzubiella, J.; Cremer, P. S.; Jungwirth, P. Beyond the Hofmeister Series: Ion-Specific Effects on Proteins and Their Biological Functions. *J. Phys. Chem. B* **2017**, *121*, 1997−2014.
(54) Ghosh, T.; García, A. E.; Garde, S. Water-Mediated Three-Particle Interactions between Hydrophobic Solutes: Size, Pressure , and Salt Effects. *J. Phys. Chem. B* **2003**, *107*, 612−617.
(55) Frank, H. S.; Evans, M. W. Free Volume and Entropy in Condensed Systems III. Entropy in Binary Liquid Mixtures. *J. Chem. Phys.* **1945**, *13*, 507−532.
(56) Chandler, D. Interfaces and the Driving Force of Hydrophobic Assembly. *Nature* **2005**, *437*, 640−647.
(57) Meyer, E. E.; Rosenberg, K. J.; Israelachvili, J. Recent Progress in Understanding Hydrophobic Interactions. *Proc. Natl. Acad. Sci. U.S.A.* **2006**, *103*, 15739−15746.
(58) Urbic, T.; Dill, K. A. Analytical Theory of the Hydrophobic Effect of Solutes in Water. *Phys. Rev. E* **2017**, *96*, 032101.
(59) Zangi, R.; Hagen, M.; Berne, B. J. Effect of Ions on the Hydrophobic Interaction between Two Plates. *J. Am. Chem. Soc.* **2007**, *129*, 4678−4686.
(60) Heyda, J.; Okur, H. I.; Hladílková, J.; Rembert, K. B.; Hunn, W.; Yang, T.; Dzubiella, J.; Jungwirth, P.; Cremer, P. S. Guanidinium can both Cause and Prevent the Hydrophobic Collapse of Biomacromolecules. *J. Am. Chem. Soc.* **2017**, *139*, 863−870.
(61) Nezafati, N.; Moztarzadeh, F.; Hesaraki, S. Surface Reactivity and in vitro Biological Evaluation of Sol Gel Derived Silver/calcium Silicophosphate Bioactive Glass. *Biotechnol. Bioprocess Eng.* **2012**, *17*, 746−754.
(62) Jorgensen, W. L.; Chandrasekhar, J.; Madura, J. D.; Impey, R. W.; Klein, M. L. Comparison of Simple Potential Functions for Simulating Liquid Water. *J. Chem. Phys.* **1983**, *79*, 926−935.
(63) Horn, H. W.; Swope, W. C.; Pitera, J. W.; Madura, J. D.; Dick, T. J.; Hura, G. L.; Head-Gordon, T. Development of an Improved Four-Site Water Model for Biomolecular Simulations: TIP4P-Ew. *J. Chem. Phys.* **2004**, *120*, 9665−9678.
(64) Darden, T.; York, D.; Pedersen, L. Particle Mesh Ewald: An N·log(N) Method for Ewald Sums in Large Systems. *J. Chem. Phys.* **1993**, *98*, 10089−10092.
(65) Case, D. A.; Betz, R. M.; Botello-Smith, W.; Cerutti, D. S.; Cheatham, T. E., III, Darden, T. A.; Duke, R. E.; Giese, T. J.; Gohlke, H.; Goetz, A. W.; et al. *Amber 16*; University of California: San Francisco, 2016.
(66) Kumar, S.; Rosenberg, J. M.; Bouzida, D.; Swendsen, R. H.; Kollman, P. A. The Weighted Histogram Analysis Method for Free-energy Calculations on Biomolecules. I. The Method. *J. Comput. Chem.* **1992**, *13*, 1011−1021.

https://dx.doi.org/10.1021/acs.jpcb.0c06399
J. Phys. Chem. B 2020, 124, 10326−10336

(67) Kumar, S.; Rosenberg, J. M.; Bouzida, D.; Swendsen, R. H.; Kollman, P. A. Multidimensional Free-energy Calculations Using the Weighted Histogram Analysis Method. *J. Comput. Chem.* **1995**, *16*, 1339−1350.
(68) Zieba, K.; Czaplewski, C.; Liwo, A.; Graziano, G. Hydrophobic Hydration and Pairwise Hydrophobic Interaction of Lennard-Jones and Mie Particles in Different Water Models. *Phys. Chem. Chem. Phys.* **2020**, *22*, 4758−4771.
(69) Makowski, M.; Sobolewski, E.; Czaplewski, C.; Ołdziej, S.; Liwo, A.; Scheraga, H. A. Simple Physics-Based Analytical Formulas for the Potentials of Mean Force for the Interaction of Amino Acid Side Chains in Water. IV. Pairs of Different Hydrophobic Side Chains. *J. Phys. Chem. B* **2008**, *112*, 11385−11395.
(70) Ben-Amotz, D. Hydrophobic Ambivalence: Teetering on the Edge of Randomness. *J. Phys. Chem. Lett.* **2015**, *6*, 1696−1701.
(71) Xie, W.-H.; Shiu, W.-Y.; Mackay, D. A Review of the Effects of Salts on the Solubility of Organic Compunds in Seawater. *Mar. Environ. Res.* **1997**, *44*, 429−444.
(72) McDevit, W. F.; Long, F. A. The Acitivity Coefficient of Benzene in Aqueous Salt Solutions. *J. Am. Chem. Soc.* **1952**, *74*, 1773−1777.
(73) Izadi, S.; Aguilar, B.; Onufriev, A. V. Protein-Ligand Electrostatic Binding Free Energies from Explicit and Implicit Solvation. *J. Chem. Theory Comput.* **2015**, *11*, 4450−4459.
(74) Vega, C.; Abascal, J. L. F. Physical Chemistry Chemical Physics Influence of Water-Protein Hydrogen Bonding on the Stability of Trp-Cage Miniprotein Simulating Water with Rigid Non-Polarizable Models: A General Perspective. *Phys. Chem. Chem. Phys.* **2011**, *13*, 19663−19688.
(75) Mobley, D. L.; Bayly, C. I.; Cooper, M. D.; Shirts, M. R.; Dill, K. A. Small Molecule Hydration Free Energies in Explicit Solvent: An Extensive Test of Fixed-Charge Atomistic Simulations. *J. Chem. Theory Comput.* **2009**, *5*, 350−358.
(76) Nayar, D.; Chakravarty, C. Sensitivity of local hydration behaviour and conformational preferences of peptides to choice of water model. *Phys. Chem. Chem. Phys.* **2014**, *16*, 10199−10213.

https://dx.doi.org/10.1021/acs.jpcb.0c06399
J. Phys. Chem. B 2020, 124, 10326−10336